Effects of Liquid Distribution on Flame Spread over Porous Solid Soaked with Combustible Liquid

Kazunori KUWANA, Masataro SUZUKI, Ritsu DOBASHI, and Toshisuke HIRANO
Department of Chemical System Engineering
School of Engineering
The University of Tokyo
7-3-1 Hongo, Bunkyo-ku, Tokyo 113-8656, JAPAN

ABSTRACT

Effects of phase change on the flame spread over the porous solid soaked with a combustible liquid has been analyzed for the case when the main mode of heat transfer is conduction. In the model, the fuel-soaked layer is assumed to be divided into three regions: liquid-solid region; three-phase region; vapor-solid region. It is shown that the flame spread rate increases with the thickness of three-phase region. The thickness of the three-phase region increases with the decrease of the diameter of solid particles because of the capillary effects. These results imply that the flame spread rate decreases with the increase of the diameter of solid particles. Thus, the decreasing tendency of the flame spread rate can be explained. The flame behavior as well as the temperature distributions predicted in the present study fairly well coincide with the experimental results, and the model developed here is shown to be valid.

KEY WORDS: Flame Spread; Liquid Soaked Solid Bed; Oil Fire

NOMENCLATURE

c	Thickness parameter of vapor-solid region.
Δc	Thickness parameter of three-phase region.
d	Diameter of solid particles.
f_1, f_2	Location functions of interface.
g	Gravitational acceleration.
Δh_{vap}	Latent heat of evaporation.
K	Permeability.
K_r	Relative permeability.
P_c	Capillary pressure.

q	Heat flux.
s	Scaled liquid saturation.
T	Temperature.
T_∞	Initial temperature.
T_b	Boiling temperature of liquid.
T_s	Surface temperature.
V_f	Flame spread rate.
x, y	Cartesian coordinates.

Greek symbols

α	Thermal diffusivity.
δ	One-dimensional thickness of three-phase region.
η, ξ	Parabolic-cylinder coordinates.
ε	Porosity.
ϕ	Parameter in Eq. (4).
κ	Parameter in Eq. (4).
λ	Thermal conductivity.
ν	Kinematic viscosity.
ρ	Density.

Subscripts

liq	Liquid.
vap	Vapor.
l	Liquid-solid region.
v	Vapor-solid region.
t-p	Three-phase region.

INTRODUCTION

In the case when a combustible liquid is accidentally spilled, it most likely soaks into a porous solid such as sand, soil, mat, or carpet. If a fire occurs, a flame will spread over the porous solid soaked with a combustible liquid. The characteristics of the flame spread phenomena, in such a case, are extremely different from those of the flame spread over a pure liquid pool. The main cause of such differences is attributable to the behavior of the liquid in solid phase [1-5].

Takeno and Hirano performed experimental studies [1-3] of the flame spread over glass beads soaked with n-decane whose flash point is 46°C. They found that the flame spread rate V_f depends significantly on the diameter d of solid particles as shown in Fig. 1 [2]. For an initial

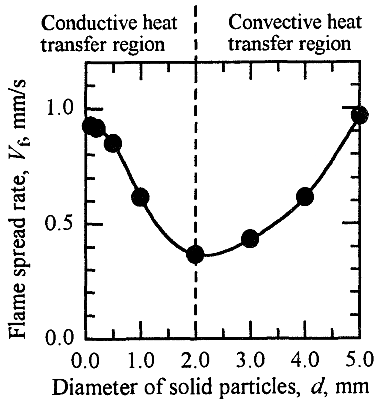

FIGURE 1 Dependence of flame spread rate on the diameter of solid particles [2].

liquid temperature much lower than its flash point, preheating of the liquid ahead of the leading flame edge is needed for flame spreading because the concentration of the combustible vapor ahead of the leading flame edge is not sufficient for burning. This preheating process plays a significant role in the flame spread phenomena. In the case to be examined in this study, it can be considered that the heat transfer to the liquid ahead of the leading flame edge mainly occurs through the fuel-soaked layer.

In the previous studies, it was attempted to explore the mechanisms of the heat transfer process through the fuel-soaked layer. For large solid particles, a liquid flow induced by buoyancy and surface tension was observed, and the main mode of heat transfer was shown to be convection. The aspects of flame spread were well explained on the basis of convective heat transfer [2, 5]. For small solid particles, on the other hand, a liquid flow was scarcely induced and the main mode of heat transfer was assumed to be conduction. Moreover, phase of the fuel changes in the porous solid bed [2-4] as shown in Fig. 2. In such a case, the major driving forces of the liquid motion are gravitational force and capillary force. The latter depends on the diameter of solid particles d. Thus, the distribution of the liquid depends on d, and surely affects the heat transfer through the fuel-soaked layer [2, 3]. However, there still

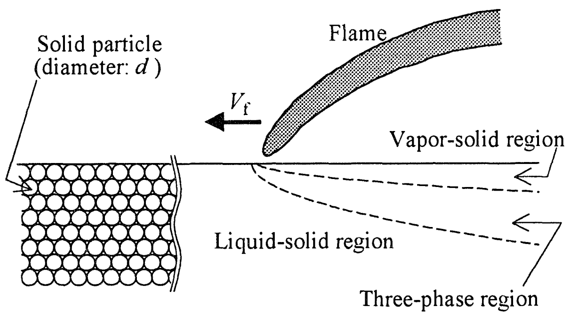

FIGURE 2 Phase change in porous solid bed.

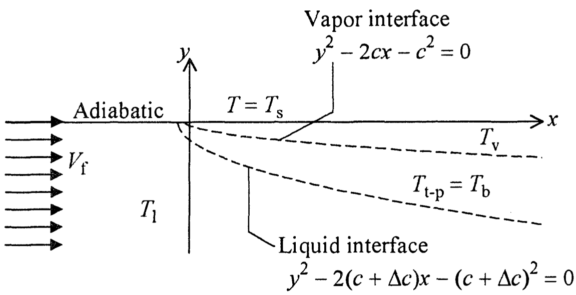

FIGURE 3 Schematic of the model. Coordinates are fixed at the leading flame edge.

remain a lot of ambiguities in the flame spread process in such a case because of the complexity of the liquid behavior.

In the present study, the temperature distribution in the fuel-soaked layer is analyzed, and the effects of the liquid distribution on the flame spread rate are investigated in order to understand the mechanisms of flame spread when the main mode of heat transfer is conduction.

FORMULATION OF PROBLEM

Model

Figure 3 shows a schematic of the present model. The coordinates are fixed at the leading flame edge, so that the fuel-soaked layer moves at a velocity of V_f in the direction opposed to the flame spread. Since the purpose of this study is to explore the effects of the liquid distribution in the fuel-soaked layer on flame spread phenomena, the influence of gas phase is simulated by prescribing thermal boundary conditions at the surface of the fuel-soaked layer, as adopted by Torrance [6] and Torrance and Mahajan [7, 8] for numerical simulations of flame spread over a pure liquid pool.

In the case to be examined here, the dominant mode of heat transfer is conduction, and the convection is negligible. Therefore, the heat transfer mechanisms are considered to be similar with those of the flame spread over a solid material. De Ris [9] developed a flame spread formula which relates the flame spread rate to the solid and gas phase properties. He assumed a constant temperature at the solid surface, and his formula well explains flame spread phenomena qualitatively. After his study, some researchers developed models which assume a constant temperature at the fuel surface [10-12]. The model developed here also adopts the same assumption. Furthermore, the surface of the fuel-soaked layer ahead of the flame ($x < 0$) is assumed adiabatic because significant heat exchange between the gas phase and the fuel-soaked layer is not expected to occur until they reach just below the leading flame edge.

In the fuel-soaked layer, three regions are assumed to exist: liquid-solid region; three-phase (liquid, vapor, and solid) region; vapor-solid region. For the liquid interface and the vapor interface, parabolic shape is assumed. The location of the vapor interface is expressed as $f_1(x, y) = y^2 - 2cx - c^2 = 0$, and that of the liquid interface as $f_2(x, y) = y^2 - 2(c + \Delta c)x - (c + \Delta c)^2 = 0$. The c and Δc are parameters which represent the thickness of the vapor-solid region and that of the three-phase region, respectively.

Bau and Torrance [13] and Udell [14] performed experiments on the boiling of liquid in the porous media. These experiments show that the temperature of the three-phase region is almost constant. In this study, following their results, the temperature of the three-phase region is assumed constant at the boiling temperature T_b of liquid.

The constant properties for each region are assumed. Although the effects of property variation can be important for advanced predictions, this assumption is reasonable in the model firstly developed for predicting the flame spread phenomena over liquid soaked porous solid. The property variations are not so large in the range of conditions interested in this study.

Major assumptions adopted here on the basis of the above discussion are summarized as follows:
1) The convective heat transfer in the fuel-soaked layer is negligible.
2) The surface temperature is constant beneath the flame, and the layer surface is adiabatic ahead of the flame.
3) The fuel-soaked layer is divided into three as: liquid-solid region; three-phase region; vapor-solid region. The shape of each interface is parabolic.
4) The temperature of the three-phase region is constant at the boiling temperature of the liquid.
5) The properties of each region are constant.

Basic Equations

Based on assumptions mentioned above, the following set of steady-state equations for energy conservation is introduced:
Liquid-solid region:

$$\frac{V_{\mathrm{f}}}{\alpha_{\mathrm{l}}}\frac{\partial T_{\mathrm{l}}}{\partial x}=\frac{\partial^2 T_{\mathrm{l}}}{\partial x^2}+\frac{\partial^2 T_{\mathrm{l}}}{\partial y^2}, \tag{1}$$

Three-phase region:

$$T_{\text{t-p}}=T_{\mathrm{b}}, \tag{2}$$

Vapor-solid region:

$$\frac{V_{\mathrm{f}}}{\alpha_{\mathrm{v}}}\frac{\partial T_{\mathrm{v}}}{\partial x}=\frac{\partial^2 T_{\mathrm{v}}}{\partial x^2}+\frac{\partial^2 T_{\mathrm{v}}}{\partial y^2}, \tag{3}$$

where α denotes the thermal diffusivity, and subscripts l, t-p, and v denote the liquid-solid region, three-phase region, and vapor-solid region, respectively.

Heat transfer in the solid-particle bed soaked with fluid occurs through both fluid in the void space and solid phase [3, 15]. In such a case, the effective thermal conductivity λ_{eff} of the mixture of the fluid and solid particles, for close packing of spheres, is expressed as [15]:

$$\lambda_{\text{eff}} = \varepsilon\lambda_{\text{fluid}} + \frac{0.895(1-\varepsilon)}{(2/3)\kappa + \phi(\kappa)}\lambda_{\text{fluid}}, \ \kappa = \lambda_{\text{solid}} / \lambda_{\text{fluid}}, \tag{4}$$

where ε is the porosity of the particle bed, and ϕ, which is a function of κ, is a parameter that represents the effective thickness of the fluid film in the void space. In the present study, Eq. (4) is used for estimation of thermal properties of the liquid-solid region and the vapor-solid region.

Boundary Conditions

The following boundary conditions for T_{l} and T_{v} are adopted in the present analysis.
At the surface of the fuel-soaked layer ($y = 0$):

$$\frac{\partial T_{\text{l}}}{\partial y} = \frac{\partial T_{\text{v}}}{\partial y} = 0 \quad \text{for } x < 0, \tag{5}$$

$$T_{\text{v}} = T_{\text{s}} \quad \text{for } x \geq 0, \tag{6}$$

where T_{s} denotes the constant temperature at the surface of the fuel-soaked layer.
At far upstream ($x = -\infty$):

$$T_{\text{l}} = T_{\infty}, \tag{7}$$

where T_{∞} denotes the initial temperature.
At far downstream ($x = \infty$):

$$\frac{\partial T_{\text{l}}}{\partial x} = \frac{\partial T_{\text{v}}}{\partial x} = 0. \tag{8}$$

At far below the surface ($y = -\infty$):

$$T_{\text{l}} = T_{\infty}. \tag{9}$$

At vapor interface ($y^2 - 2cx - c^2 = 0$):

$$T_{\text{v}} = T_{\text{b}}. \tag{10}$$

At liquid interface ($y^2 - 2(c + \Delta c)x - (c + \Delta c)^2 = 0$):

$$T_{\text{l}} = T_{\text{b}}. \tag{11}$$

Finally, the energy balance through the three-phase region is required. The liquid vaporizes through the three-phase region. Therefore, the heat from the vapor-solid region into the three-phase region is partly consumed in the three-phase region due to evaporation and conducts into the liquid-solid region. Considering that the heat transfer occurs only in the x-direction at the layer surface, the energy balance through the three-phase region at $y = 0$ yields:

$$\lambda_\mathrm{v} \frac{\partial T_\mathrm{v}}{\partial x}\left(-\frac{c}{2}, 0\right) = \lambda_\mathrm{l} \frac{\partial T_\mathrm{l}}{\partial x}\left(-\frac{c+\Delta c}{2}, 0\right) + \varepsilon \rho_\mathrm{liq} V_\mathrm{f} \Delta h_\mathrm{vap}, \tag{12}$$

where ρ_liq and Δh_vap denote the density of liquid and latent heat of evaporation, respectively.

RESULTS AND DISCUSSION

Solutions in Parabolic-Cylinder Coordinates

The following parabolic-cylinder coordinates are introduced [11] to solve Eqs. (1) and (3):

$$x = \frac{1}{2}\left(\xi^2 - \eta^2\right),\ y = \xi\eta. \tag{13}$$

In terms of η and ξ, Eqs. (1) and (3) are rewritten as:

$$\frac{V_\mathrm{f}}{\alpha_\mathrm{l}}\left(\xi \frac{\partial T_\mathrm{l}}{\partial \xi} - \eta \frac{\partial T_\mathrm{l}}{\partial \eta}\right) = \frac{\partial^2 T_\mathrm{l}}{\partial \xi^2} + \frac{\partial^2 T_\mathrm{l}}{\partial \eta^2}, \tag{14}$$

$$\frac{V_\mathrm{f}}{\alpha_\mathrm{v}}\left(\xi \frac{\partial T_\mathrm{v}}{\partial \xi} - \eta \frac{\partial T_\mathrm{v}}{\partial \eta}\right) = \frac{\partial^2 T_\mathrm{v}}{\partial \xi^2} + \frac{\partial^2 T_\mathrm{v}}{\partial \eta^2}. \tag{15}$$

Boundary conditions are also rewritten in terms of η and ξ as:

$$T_\mathrm{v} = T_\mathrm{s} \qquad \text{at } \eta = 0, \tag{16}$$

$$T_\mathrm{v} = T_\mathrm{b} \qquad \text{at } \eta = \sqrt{c}, \tag{17}$$

$$T_\mathrm{l} = T_\mathrm{b} \qquad \text{at } \eta = \sqrt{c + \Delta c}, \tag{18}$$

$$T_\mathrm{l} = T_\infty \qquad \text{at } \eta = \infty, \tag{19}$$

$$\frac{\partial T_\mathrm{l}}{\partial \xi} = \frac{\partial T_\mathrm{v}}{\partial \xi} = 0 \qquad \text{at } \xi = 0, \tag{20}$$

$$\frac{\partial T_\mathrm{l}}{\partial \xi} = \frac{\partial T_\mathrm{v}}{\partial \xi} = 0 \qquad \text{at } \xi = -\infty. \tag{21}$$

The boundary conditions (20) and (21) indicate that the T_l and T_v are independent of ξ. Therefore, Eqs. (14) and (15) reduce to the ordinary differential equations as:

$$\frac{V_{\mathrm{f}}}{\alpha_{\mathrm{l}}}\eta\frac{\mathrm{d}T_{\mathrm{l}}}{\mathrm{d}\eta}+\frac{\mathrm{d}^2T_{\mathrm{l}}}{\mathrm{d}\eta^2}=0, \tag{22}$$

$$\frac{V_{\mathrm{f}}}{\alpha_{\mathrm{v}}}\eta\frac{\mathrm{d}T_{\mathrm{v}}}{\mathrm{d}\eta}+\frac{\mathrm{d}^2T_{\mathrm{v}}}{\mathrm{d}\eta^2}=0. \tag{23}$$

Solution of Eqs. (22) and (23) with boundary conditions (16) through (19) yields:

$$T_{\mathrm{l}}=T_{\infty}+\left(T_{\mathrm{b}}-T_{\infty}\right)\frac{\mathrm{erfc}\left(\sqrt{V_{\mathrm{f}}/2\alpha_{\mathrm{l}}}\,\eta\right)}{\mathrm{erfc}\left(\sqrt{V_{\mathrm{f}}(c+\Delta c)/2\alpha_{\mathrm{l}}}\right)}, \tag{24}$$

$$T_{\mathrm{v}}=T_{\mathrm{b}}+\left(T_{\mathrm{s}}-T_{\mathrm{b}}\right)\left\{1-\frac{\mathrm{erf}\left(\sqrt{V_{\mathrm{f}}/2\alpha_{\mathrm{v}}}\,\eta\right)}{\mathrm{erf}\left(\sqrt{V_{\mathrm{f}}c/2\alpha_{\mathrm{v}}}\right)}\right\}. \tag{25}$$

Transforming Eq. (12) into that on the η-ξ coordinates along with Eqs. (24) and (25), the following relation is obtained:

$$\begin{aligned}&\lambda_{\mathrm{l}}\sqrt{\frac{2V_{\mathrm{f}}}{\pi(c+\Delta c)\alpha_{\mathrm{l}}}}\frac{T_{\mathrm{b}}-T_{\infty}}{\mathrm{erfc}\left(\sqrt{V_{\mathrm{f}}(c+\Delta c)/2\alpha_{\mathrm{l}}}\right)}\exp\left\{-\frac{V_{\mathrm{f}}(c+\Delta c)}{2\alpha_{\mathrm{l}}}\right\}+\varepsilon\rho_{\mathrm{liq}}V_{\mathrm{f}}\Delta h_{\mathrm{vap}}\\&\quad=\lambda_{\mathrm{v}}\sqrt{\frac{2V_{\mathrm{f}}}{\pi c\alpha_{\mathrm{v}}}}\frac{T_{\mathrm{s}}-T_{\mathrm{b}}}{\mathrm{erf}\left(\sqrt{V_{\mathrm{f}}c/2\alpha_{\mathrm{v}}}\right)}\exp\left(-\frac{V_{\mathrm{f}}c}{2\alpha_{\mathrm{v}}}\right).\end{aligned} \tag{26}$$

Equation (26) relates the flame spread rate to the c and Δc, those are the parameters of the liquid distribution in the fuel-soaked layer. Figure 4 shows a typical temperature field of the fuel-soaked layer predicted in the present study. The parameters adopted for Fig. 4 are listed in Table 1. The c, Δc, and V_{f} in Table 1 satisfy the relationship of Eq. (26).

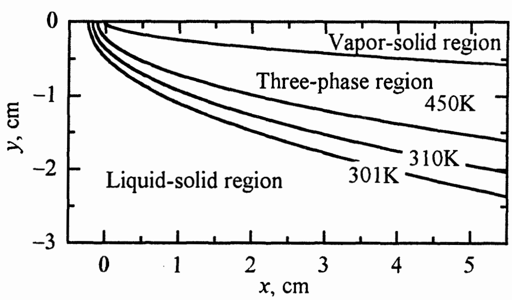

FIGURE 4 Typical temperature field predicted in the present study.

TABLE 1 Parameters adopted in Fig. 4.

T_∞	T_b	T_s	ρ_{liq}	Δh_{vap}	ε	λ_l
300 K	450 K	1000 K	730 kg/m^3	276 kJ/kg	0.26	0.4 W/mK

λ_v	$\alpha_l \times 10^7$	$\alpha_v \times 10^7$	$V_f \times 10^4$	c	Δc
0.2 W/mK	2.5 m^2/s	4.0 m^2/s	9.17 m/s	0.3 mm	2 mm

Effects of Liquid Distribution on Flame Spread Rate

By solving Eq. (26) numerically, the flame spread rate is expressed as a function of the c and Δc. Figure 5 shows V_f as a function of Δc, with c as a parameter. In the limiting case of $\Delta c = 0$, that means the three-phase region does not exist, V_f is proportional to c^{-1} if other parameters are retained constant [11]. It is shown that the flame spread rate decreases with the increase of c, the thickness of the vapor-solid region. To the contrary, V_f increases with the increase of Δc, the thickness of the three-phase region. Especially, V_f increases sharply with a little increase of Δc from zero. Thus, it is found that effects of the three-phase region on the flame spread rate cannot be ignored.

Dependence of Particle Size on Liquid Distribution

The thickness of the three-phase region depends on the balance between the capillary force and gravitational force [13, 14]. The capillary force is a function of the diameter of solid particles. Therefore, the thickness of the three-phase region significantly depends on the diameter of solid particles. Udell [14] developed the formula which relates the thickness δ of the three-phase region to the properties of the liquid, vapor, and solid by using a one-dimensional model. His model considers the effects of the capillary force, gravitational force, and the phase change due to the evaporation. In the case when the porous media is heated from its top, the result of the one-dimensional analysis yields [14]:

$$\delta = \int_{s=0}^{s=1} \frac{P_c}{(\rho_{liq} - \rho_{vap})g + \dfrac{q}{\Delta h_{vap}} \dfrac{1}{K} \left(\dfrac{\nu_{vap}}{K_{rvap}} + \dfrac{\nu_{liq}}{K_{rliq}} \right)} ds, \tag{27}$$

where P_c, g, q, K, K_r, ν, and s denote the capillary pressure, gravitational acceleration, heat flux, permeability, relative permeability, kinematic viscosity, and scaled liquid saturation, respectively. The subscripts liq and vap denote the liquid and vapor phase, respectively. From Eq. (27), the thickness of the three-phase region increases with the decrease of the density or kinematic viscosity of the liquid. Both K and P_c are the functions of the diameter d of solid

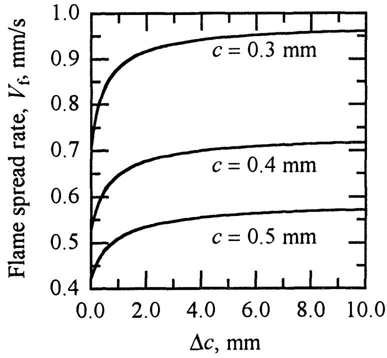

FIGURE 5 Effects of region thickness on flame spread rate.

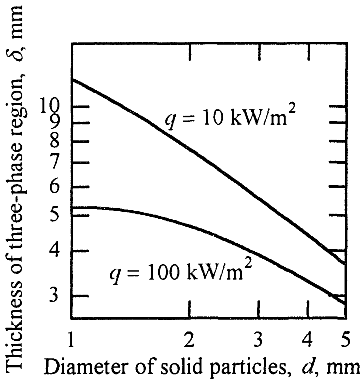

FIGURE 6 Thickness of three-phase region as a function of d. This is obtained by one-dimensional analysis [14].

particles, and each dependence on d is expressed as follows:

$$K \propto d^2, \tag{28}$$

$$P_c \propto K^{-1/2} \propto d^{-1}. \tag{29}$$

Figure 6 shows δ as a function of d, with q as a parameter for $1 \leq d \leq 5$ mm. The integration of the right hand side of Eq. (27) was performed by using a fourth-order Runge-Kutta algorithm. According to Fig. 6, it is found that the thickness of three phase region significantly depends on d and decreases with the increase of d for the range examined in the present study. As mentioned above, the flame spread rate increases with the thickness of three-phase region (Fig. 5). From these results, the tendency that V_f decreases with the increase of d (Fig. 1) can be explained by considering the capillary effect on the thickness of three-phase region.

Temperature Profiles

Figure 7 shows the temperature profiles at $y = -5$ mm predicted in the present study. In the same figure, the experimental results measured by Takeno and Hirano [1] are also plotted. Calculation results agree well with the experimental results. This agreement implies that the dominant mode of the heat transfer in the liquid-solid region is conduction, and the assumptions adopted in the present study is considered to be valid. In Fig. 7, the measured temperature is a little higher than the predicted temperature for $x < 1$ cm. This difference is considered to be attributable to the heat flux from the gas phase into the fuel-soaked layer at the layer surface which is neglected in the present study.

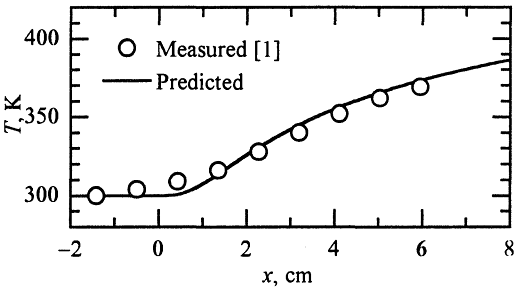

FIGURE 7 Temperature profiles in the liquid-solid region at $y = -5$ mm.

CONCLUSIONS

An analytical study of effects of the liquid distribution on the flame spread over the porous solid soaked with a combustible liquid has been performed for the case when the dominant mode of heat transfer is conduction. Main conclusions derived throughout this study are as follows:

1) The flame spread rate is predicted to decrease with the increase of the thickness of the vapor-solid region and to increase with that of three-phase region.
2) Predicted temperature profiles coincide fairly well with those examined in previous experimental study.
3) The model developed through the present study provides a means to predict the relationship between the flame spread rate and the liquid distribution in a bed of porous solid soaked with combustible liquids.

REFERENCES

1. Takeno, K. and Hirano, T., "Flame Spread over Porous Solids Soaked with a Combustible Liquid", Twenty-fist Symposium (International) on Combustion, The Combustion Institute, 75-81, 1986.

2. Takeno, K. and Hirano, T., "Behavior of Combustible Liquid Soaked in Porous Beds during Flame Spread", Twenty-second Symposium (International) on Combustion, The Combustion Institute, 1223-1230, 1988.

3. Takeno, K, "Study on Flame Spread over Surface of Mixture of Solid and Combustible Liquid", Ph.D. Thesis, The University of Tokyo, 1989.

4. Ishida, H., "Flame Spread over Fuel-Soaked Ground", Fire Safety Journal, 10, 163-171, 1986.

5. Kuwana, K., Suzuki, M., Dobashi, R., and Hirano, T., "Numerical Simulation of

Combustible Liquid Behavior and Temperature Distribution in a Solid-Liquid Mixed Layer during Flame Spread over It", Fire Safety Science - Proceedings of the 5th International Symposium, 367-378, 1997.

6. Torrance, K. E., "Subsurface Flows Preceding Flame Spread over a Liquid Fuel", Combustion Science and Technology, 3, 133-143, 1971.

7. Torrance, K. E. and Mahajan, R. L., "Fire Spread over Liquid Fuels: Liquid Phase Parameters", Fifteenth Symposium (International) on Combustion, The Combustion Institute, 281-287, 1974.

8. Torrance, K. E. and Mahajan, R. L., "Surface Tension Flows Induced by a Moving Thermal Source", Combustion Science and Technology, 10, 125-136, 1975.

9. de Ris, J. N., "Spread of a Laminar Diffusion Flame", Twelfth Symposium (International) on Combustion, The Combustion Institute, 241-252, 1969.

10. Wichman, I. S. and Williams, F. A., "A Simplified Model of Flame Spread in an Opposed Flow along a Flat Surface of a Semi-Infinite Solid", Combustion Science and Technology, 32, 91-123, 1983.

11. Atreya, A., "Steady Propagation of an Opposed-Wind Diffusion Flame on a Charring Solid", Proceedings of the Eighth International Heat Transfer Conference, 849-856, 1986.

12. Bhattacharjee, S., West, J., and Dockter, S., "A Simplified Theory for de Ris Flame over Thick and Thin Fuel Beds", Combustion and Flame, 104, 66-80, 1996.

13. Bau, H. H. and Torrance, K. E., "Boiling in Low-Permeability Porous Materials", International Journal of Heat and Mass Transfer, 25, 45-55, 1982.

14. Udell, K. S., "Heat Transfer in Porous Media Considering Phase Change and Capillarity – the Heat Pipe Effect", International Journal of Heat Mass Transfer, 28, 485-495, 1985.

15. Kunii, D. and Smith, J. M., "Heat Transfer Characteristics of Porous Rocks", AIChE Journal, 6, 71-78, 1960.